

Inhomogeneous phases in the quark-meson model via the FRG - a status report

Part I: Flow equations with explicit inhomogeneous chiral condensates

Adrian Koenigstein & Martin J. Stein

in coorporation with: J. Braun, M. Buballa, D. H. Rischke, B.-J. Schaefer

EMMI Workshop Functional Methods in Strongly Correlated Systems
Hirschegg, April 2, 2019

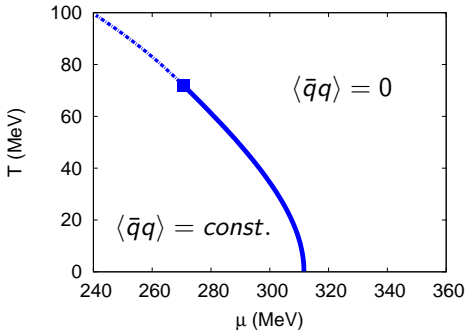


Motivation: QCD phase diagram at low T

- ▶ Standard argument for a QCD critical point:

- Lattice: crossover at high T and low μ
- Models: 1st order at low T and high μ

⇒ based on tacit assumption: $\langle \bar{q}q \rangle \cancel{\propto}$ constant in space/ homogeneous

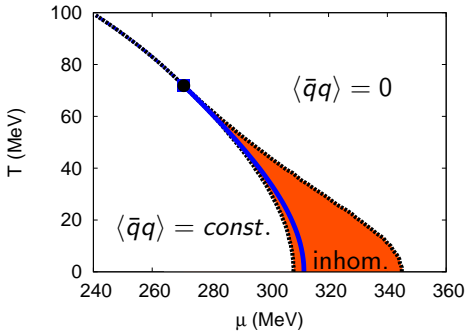


D. Nickel, Phys. Rev. D **80** 7 (2009)

Motivation: QCD phase diagram at low T

- ▶ Allowing for $\langle \bar{q}q \rangle(\vec{x}) \Rightarrow$ energetically favored inhomogeneous condensates overlapping the 1st order transition

- Critical point → Lifshitz point
- Inhomogeneous phase rather robust under model extensions and variations



D. Nickel, Phys. Rev. D **80** 7 (2009)

M. Buballa and S. Carignano, Prog. Part. Nucl. Phys. **81** (2015)

- ▶ **Current goal:** Study effects of bosonic and fermionic quantum fluctuations on inhomogeneous chiral condensates in the Quark-Meson (QM) model
 - Towards deriving, implementing and solving FRG flow equations with inhomogeneous chiral condensates (*this talk*)
 - FRG based stability analysis around the homogeneous phase (*Adrians talk on Wednesday*)
- ▶ **Method:** Study within the *Functional Renormalization Group* (FRG)
 - Highly potent tool to investigate effects of quantum fluctuations
 - In-medium computations ($T \geq 0$ and $\mu \geq 0$) are possible
 - Inclusion of inhomogeneous condensates is possible
- ▶ Part of CRC-TR 211 Project A03: Inhomogeneous phases at high density

► **Central Questions:**

1. What is the energetically preferred modulation of the chiral order parameter?
2. Are inhomogeneous phases stable under thermal and quantum fluctuations?
3. How do variations of the parameters (m_q , μ_I , μ_S , ...) influence the region of the phase diagram covered by an inhomogeneous phase and what is the order of the transition between this and the adjacent homogeneous phase?

► **Principal investigators:** Michael Buballa, Dirk H. Rischke and Marc Wagner

► **Senior collaborators:** Jens Braun, Stefan Rechenberger, Bernd-Jochen Schaefer, Lorenz von Smekal and Ralf-Arno Tripolt

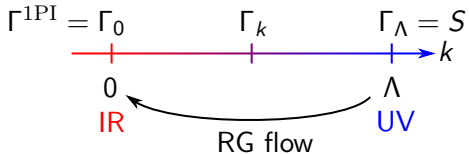
► **Researchers:** Niklas Cichutek, Taylan Erdogan, Jürgen Eser, Lutz Kiefer, Adrian Koenigstein, Dominic Kraatz, Phillip Lakaschus, Laurin Pannullo, Sabor Salek, Martin Jakob Steil and Marc Winstel

► Exact RG flow equation

$$\frac{d\Gamma_k}{dk} = \frac{1}{2} S \text{Tr} \left\{ \left[\Gamma_k^{(2)} + R_k \right]^{-1} \partial_k R_k \right\}$$



► Implementation of Wilson's RG approach:



C. Wetterich, Physics Letters B 301.1 (1993)

K. G. Wilson, Phys. Rev. B 4 9 (1971)

- Truncation of Γ_k is necessary to explicitly solve the flow equation:
Lowest-order derivative expansion: **Local potential approximation (LPA) for QM model** in the chiral limit:

$$\Gamma_{\textcolor{red}{k}}[\psi, \bar{\psi}, \phi] = \int d^4z \left\{ \bar{\psi}(z) \left[\not{\partial} - \mu \gamma_0 + g (\sigma(z) + i \gamma_5 \vec{\pi}(z)) \right] \psi(z) + \frac{1}{2} (\partial_\mu \phi(z)) (\partial^\mu \phi(z)) + U_{\textcolor{red}{k}}(\phi(z)\phi(z)) \right\}$$

- Chiral density wave (CDW) ansatz for the condensates:

$$\phi(z) \stackrel{CDW}{=} (\sigma(\vec{z}), 0, 0, \pi_3(\vec{z})) = \frac{M}{g} (\cos(\vec{q} \cdot \vec{z}), 0, 0, \sin(\vec{q} \cdot \vec{z}))$$

$$\rho(z) \equiv \phi(z)\phi(z) \stackrel{CDW}{=} \frac{M^2}{g^2} \quad \text{Spatially independent } O(4)\text{-sym. field}$$

$$\sigma(z) \pm i O \pi_3(z) \stackrel{CDW}{=} \frac{M}{g} \exp(\pm i O \vec{q} \cdot \vec{z}), \quad \text{for } O^2 = \mathbb{1} \quad \text{Euler's formula}$$

Two-point functions

► **Challenge:** Non trivial position dependence for the CDW in

$$\begin{aligned}\Gamma_k^{(0,1,1)}(x, y) &\equiv \frac{\overrightarrow{\delta}}{\delta\bar{\psi}(x)}\Gamma_k[\psi, \bar{\psi}, \phi]\frac{\overleftarrow{\delta}}{\delta\psi(y)} \\ &\stackrel{CDW}{=} \delta^{(4)}(x - y)\left[\partial_x - \gamma_0\mu + M(\cos(\vec{q} \cdot \vec{x}) + i\gamma_5\tau_3 \sin(\vec{q} \cdot \vec{x}))\right] \\ &= \delta^{(4)}(x - y)\left[\partial_x - \gamma_0\mu + M \exp(i\gamma_5\tau_3\vec{q} \cdot \vec{x})\right]\end{aligned}$$

$$\begin{aligned}\Gamma_k^{(2,0,0)}(x, y) &\equiv \frac{\delta}{\delta\phi_i(x)}\frac{\delta}{\delta\phi_j(y)}\Gamma_k[\psi, \bar{\psi}, \phi] \\ &\stackrel{CDW}{=} \delta^{(4)}(x - y)\left[\left(-\partial_x^2 + 2U'_k(\rho)\right)\delta_{ij} + 4U''_k(\rho)\phi_i(x)\phi_j(x)\right]\end{aligned}$$

► **Solution:** Construct unitary transformation ($U^\dagger U = \mathbb{1}$ and $\partial_k U = 0$) for the CDW analytically to eliminate explicit position dependence \Leftrightarrow diagonalize $\Gamma_k^{(2)}$ in momentum space

Unitary transformations for the CDW

► The transformation for the fermionic two-point function:

$$U_F(\vec{x}) \equiv \exp\left(-\frac{i}{2}\gamma_5\tau_3\vec{q} \cdot \vec{x}\right)$$

diagonalizes $\gamma_0\Gamma_k^{(0,1,1)}$ in momentum space:

$$\begin{aligned}\tilde{\Gamma}_{k;U}^{(0,1,1)}(p,r) &\equiv \int \frac{d^4 p'}{(2\pi)^4} \int \frac{d^4 p''}{(2\pi)^4} U^\dagger(p,p') \gamma_0 \Gamma_k^{(0,1,1)}(p',p'') U(p'',r) \\ &= (2\pi)^4 \delta^{(4)}(p-r) \left[ip_0 - \mu + i\gamma_0\gamma_i p^i + \frac{i}{2} \gamma_0 \gamma_5 \tau_3 \gamma_i q^i + \gamma_0 M \right].\end{aligned}$$

► The transformation for the bosonic two-point function:

$$U_B(\vec{x}) \equiv \frac{1}{2} \begin{pmatrix} 1 - \exp(-2i\vec{q} \cdot \vec{x}) & 0 & 0 & 1 + \exp(-2i\vec{q} \cdot \vec{x}) \\ 0 & 2 & 0 & 0 \\ 0 & 0 & 2 & 0 \\ -i(1 + \exp(-2i\vec{q} \cdot \vec{x})) & 0 & 0 & i(\exp(-2i\vec{q} \cdot \vec{x}) - 1) \end{pmatrix}.$$

diagonalizes $\Gamma_k^{(2,0,0)}$ in momentum space.

► Transformed regulators

- Generic regulators stay diagonal in momentum space under the unitary transformations U
- Example: Transformed 3D fermionic regulator

$$\begin{aligned}\tilde{R}_{k;U}^F(p, r) &\equiv \int \frac{d^4 p'}{(2\pi)^4} \int \frac{d^4 p''}{(2\pi)^4} U^\dagger(p, p') \gamma_0 R_k^F(p', p'') U(p'', r) \\ &= i(2\pi)^4 \delta^{(4)}(p - r) \sum_{\pm} P_{\pm} \gamma_0 (\vec{p} \pm \vec{q}/2) r_k^F(|\vec{p} \pm \vec{q}/2|/k),\end{aligned}$$

with the chiral projection operators $P_{\pm} \equiv \frac{1}{2} (\mathbb{1} \pm \gamma_5 \tau_3)$.

LPA Flow equation

LPA flow equation for $U_k(\rho)$ with CDW condensates

$$\begin{aligned} \partial_k U_k(\rho) = & \int \frac{d^3 p}{(2\pi)^3} \sum_{i=0}^3 \frac{1}{2} \coth \left(\frac{E_k^i}{2T} \right) \partial_k E_k^i + \\ & - 2N_c \int \frac{d^3 p}{(2\pi)^3} \sum_{\pm, \pm} \tanh \left(\frac{E_k^{\pm} \pm \mu}{2T} \right) \partial_k E_k^{\pm} \end{aligned}$$

- ▶ Using generic but **three-dimensional** FRG regulators

$$R_k^F(p, r) \equiv i \vec{p} r_k^F(|\vec{p}|/k) (2\pi)^4 \delta^{(4)}(p - r)$$

$$R_k^B(p, r) \equiv \vec{p}^2 r_k^B(|\vec{p}|/k) (2\pi)^4 \delta^{(4)}(p - r)$$

in a unified regulator scheme

$$\left(1 + r_k^F(|\vec{p}|/k) \right)^2 = 1 + r_k^B(|\vec{p}|/k) \equiv \lambda_k(|\vec{p}|)^2.$$

► **Fermionic eigenvalues:**

$$(E_k^\pm)^2 = M^2 + \frac{(\vec{p}_k^{+q})^2}{2} + \frac{(\vec{p}_k^{-q})^2}{2} + \pm \sqrt{M^2 \left(\vec{p}_k^{+q} - \vec{p}_k^{-q} \right)^2 + \frac{1}{4} \left((\vec{p}_k^{+q})^2 - (\vec{p}_k^{-q})^2 \right)^2} \\ \stackrel{q=0}{=} M^2 + (\vec{p}_k)^2$$

$$\text{with } \vec{p}_k^q \equiv (\vec{p} + \vec{q}/2)(1 + r_k^F(|\vec{p} + \vec{q}/2|/k)) = (\vec{p} + \vec{q}/2) \lambda_k(|\vec{p} + \vec{q}/2|)$$

► **Bosonic eigenvalues:**

$$(E_k^1)^2 = (E_k^2)^2 = (\vec{p}_k)^2 + 2U'_k(\rho) \stackrel{q=0}{=} (\vec{p}_k)^2 + 2U'_k(\rho) \\ (E_k^{0,3})^2 = (\vec{p}_k)^2 + \frac{1}{2}(\vec{p}_k^{+4q})^2 + 2U'_k(\rho) + 2\rho U''_k(\rho) + \\ \pm \sqrt{4\rho^2 U''_k(\rho)^2 + \frac{1}{4} \left((\vec{p}_k^{+4q})^2 - (\vec{p}_k)^2 \right)^2} \\ \stackrel{q=0}{=} (\vec{p}_k)^2 + 2U'_k(\rho) + 2\rho(U''_k(\rho) \pm |U''_k(\rho)|)$$

Mean-field approximation

- ▶ Mean-field approximation (MFA) in the present RG setting:

$$\partial_k \Gamma_k = \frac{1}{2} \left(\text{Diagram A} - \text{Diagram B} \right)$$

The equation shows the difference between two Feynman-like diagrams. Diagram A consists of two intersecting lines forming an 'X' shape, with a small circle containing a dot at their intersection point. Diagram B is a simple circle with a dot at its top, and a clockwise arrow indicating a loop.

- Neglect bosonic fluctuations and integrate the LPA flow equation

RG MFA thermodynamic potential

$$\begin{aligned} \bar{\Omega}_{\mu,T}^{\text{MFA}}(\sqrt{\rho}, q) &\equiv \frac{\Gamma_0}{V_4} = U_\Lambda(\rho) + \frac{q^2 \rho}{2} - \frac{1}{V_4} \int_{\Lambda}^0 dk \text{Diagram B} \\ &= \lambda_\Lambda (\rho - v_\Lambda^2)^2 + \frac{q^2 \rho}{2} - 2N_c \int \frac{d^3 p}{(2\pi)^3} \sum_{\pm,\pm} T \log \left[2 \cosh \left[\frac{E_k^\pm \pm \mu}{2T} \right] \right]_{k=\Lambda}^{k=0} \end{aligned}$$

Computation of phase diagrams

1. Model parameter fixation in vacuum and regulator choice
 - So far naïve parameter fixation: Fitting the quark mass M , the bare pion decay constant f_π and the sigma curvature mass m_σ in the IR
 - Exponential regulator $\lambda_k^{\text{exp}}(p)^2 = 1 + 1/(\exp(p^2/k^2) - 1)$
2. Computation of the fermionic loop at different μ , T , ρ and q
 - Numerical solution of 2D momentum integrals using the *Cubature* package¹
3. Minimization of $\bar{\Omega}_{\mu,T}(\sqrt{\rho}, q)$ to find $\Omega(\mu, T) = \bar{\Omega}_{\mu,T}(\sqrt{\rho_{\min}}, q_{\min})$
 - Minimizing a spectral decomposition in Chebyshev polynomials $T_{2n}(x)$

$$\bar{\Omega}_{\mu,T}(\sqrt{\rho}, q) = \sum_{n_1 n_2} a_{n_1 n_2}^{\mu, T} T_{2n_1}(\sqrt{\rho}) T_{2n_2}(q)$$

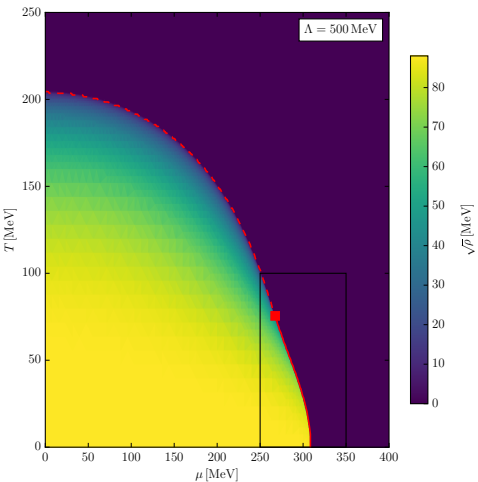
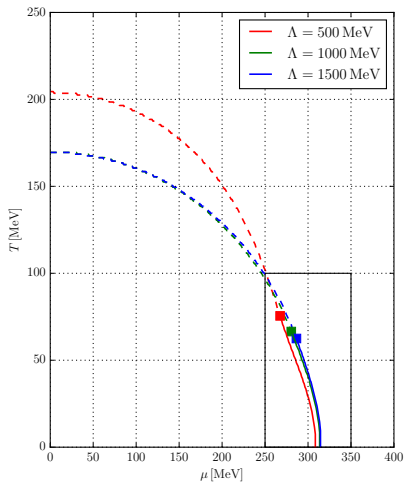
using a 2D Nelder–Mead simplex method.

4. Sampling of the μ - T -plane
 - Parallelized *Block-Structured Adaptive Mesh Refinement*

¹ *Cubature* package: github.com/stevengj/cubature

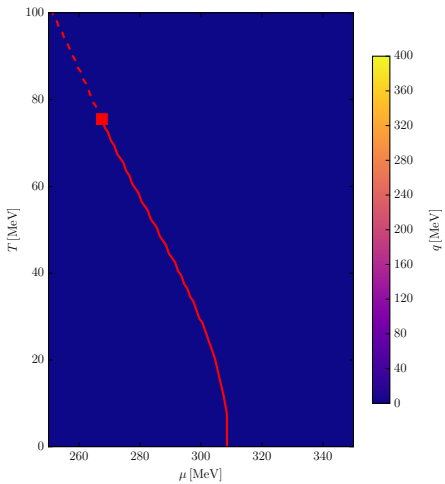
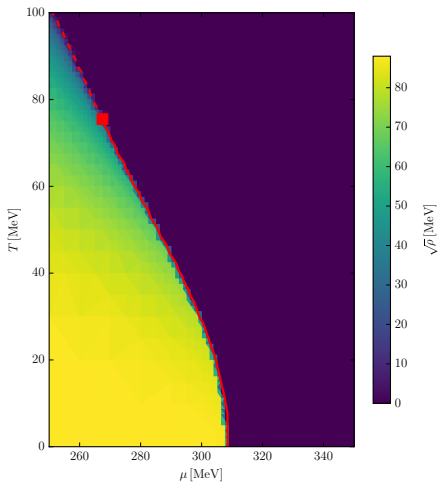
Homogeneous Mean-field phase diagrams

- ▶ λ_k^{exp} , $f_\pi = 88 \text{ MeV}$, $M = 300 \text{ MeV}$ and $m_\sigma = 600 \text{ MeV}$
- ▶ **Allowing only homogeneous condensates:** $|\vec{q}| \stackrel{!}{=} 0$



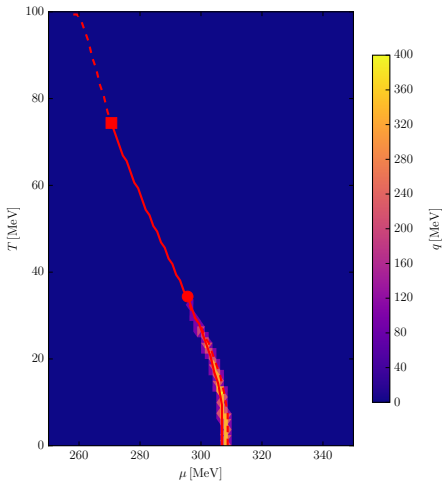
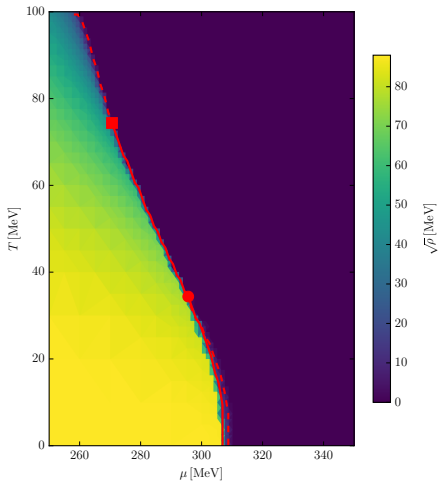
Inhomogeneous mean-field phase diagrams

- $\lambda_k^{\text{exp}}, f_\pi = 88 \text{ MeV}, M = 300 \text{ MeV}, m_\sigma = 600 \text{ MeV}$
- $\Lambda = 500 \text{ MeV}$



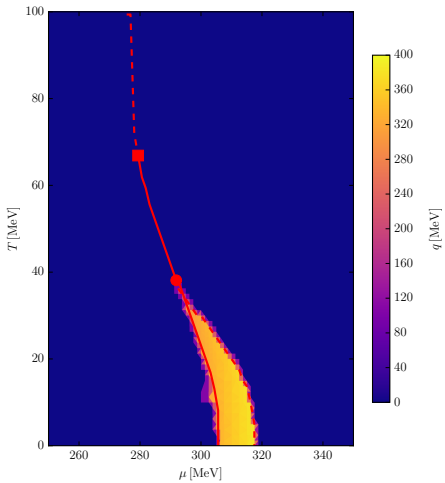
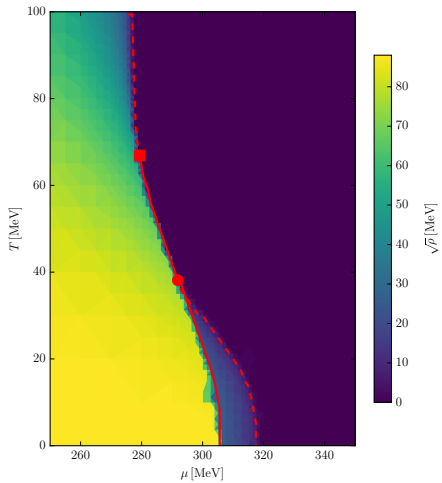
Inhomogeneous mean-field phase diagrams

- $\lambda_k^{\text{exp}}, f_\pi = 88 \text{ MeV}, M = 300 \text{ MeV}, m_\sigma = 600 \text{ MeV}$
- $\Lambda = 450 \text{ MeV}$

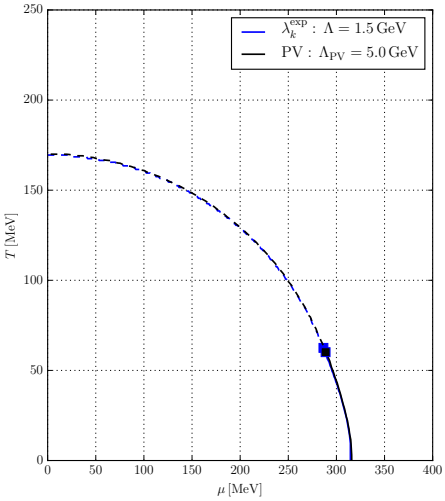


Inhomogeneous mean-field phase diagrams

- $\lambda_k^{\text{exp}}, f_\pi = 88 \text{ MeV}, M = 300 \text{ MeV}, m_\sigma = 600 \text{ MeV}$
- $\Lambda = 400 \text{ MeV}$



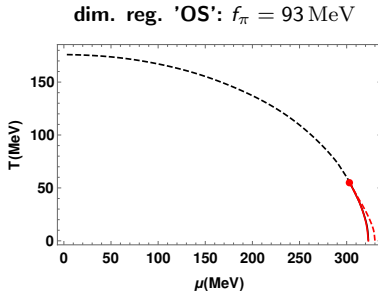
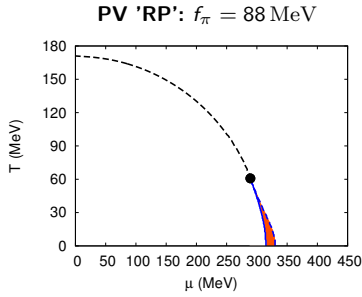
Comparison to existing hom. mean-field results



- ▶ $f_\pi = 88 \text{ MeV}$, $M = 300 \text{ MeV}$ and $m_\sigma = 2M$
- ▶ MFA with *Pauli-Villars* (PV) regularization of the vacuum term with $\Lambda_{\text{PV}} = 5.0 \text{ GeV}$ ¹
- ▶ λ_k^{exp} , naïve parameter fixation, $\Lambda = 1.5 \text{ GeV}$
- ▶ **Results are in very good agreement**

¹S. Carignano, M. Buballa, and W. Elkamhawy, Phys. Rev. D 94 3 (2016)

- ▶ Involved existing MFA results (with $M = 300 \text{ MeV}$, $m_\sigma = 2M$)
 - PV regularization and 'RP' parameter fixation at $\Lambda_{\text{PV}} = 5.0 \text{ GeV}^1$
 - Dim. regularization using the on-shell (OS) renormalization scheme²
- are in agreement and predicts a **non-vanishing inhomogeneous window**:



¹S. Carignano, M. Buballa, and W. El kamhawy, Phys. Rev. D **94** 3 (2016)

²P. Adhikari, J. O. Andersen, and P. Kneschke, Phys. Rev. D **96** 1 (2017)

Improving on the naïve RG MFA

1. *RG-consistent* MFA³ by enforcing:

$$\Lambda \frac{d\Gamma_{k=0}}{d\Lambda} = 0$$

- Initial condition $\Gamma_{\Lambda'}[\rho]$ at $\Lambda' < \Lambda$ and construction of $\Gamma_\Lambda[\rho]$ via RG-consistency
- Allows for systematic study of cutoff effects and regularization-scheme dependence
- Using a QCD motivated $\Gamma_{\Lambda'}[\rho] \propto \rho$ at $\Lambda' \sim 0.4 \dots 1.0 \text{ GeV}$?

2. Improved parameter fixation using $\Gamma_{k=0}^{(2)}$ in MFA

- Fitting to renormalized f_π
- Fitting pole-mass $m_{\sigma,p}$
- Motivated by MFA studies with Pauli-Villars regularization

³J. Braun, M. Leonhardt, and J. M. Pawłowski (2018), arXiv: 1806.04432 [hep-ph]

► What we have done so far:

- Derivation of a LPA flow eq. for inhomogeneous CDW condensates
- Development/Implementation of efficient, accurate and stable numerics
- Numerical results in naïve RG MFA

► What we are currently working on:

- Improving the naïve MFA
- Development/Implementation of numerics for the full CDW LPA flow equation in medium

► What we plan to do in the future:

- Study the effects of bosonic fluctuations using the already derived LPA flow eq. for the CDW
- Investigate the effects of different 3D (and 4D) regulators on the inhomogeneous phase
- Study cutoff effects on the inhomogeneous phase
- **Extending the truncation:** deriving flow equations beyond LPA in presence of CDW condensates

References

- D. Nickel, Phys. Rev. D **80** 7 (2009), DOI: 10.1103/PhysRevD.80.074025.
- M. Buballa and S. Carignano, Prog. Part. Nucl. Phys. **81** (2015), DOI: 10.1016/j.ppnp.2014.11.001.
- C. Wetterich, Physics Letters B **301**.1 (1993), DOI: 10.1016/0370-2693(93)90726-X.
- K. G. Wilson, Phys. Rev. B **4** 9 (1971), DOI: 10.1103/PhysRevB.4.3174.
- S. Carignano, M. Buballa, and W. Elkamhawy, Phys. Rev. D **94** 3 (2016), DOI: 10.1103/PhysRevD.94.034023.
- P. Adhikari, J. O. Andersen, and P. Kneschke, Phys. Rev. D **96** 1 (2017), DOI: 10.1103/PhysRevD.96.016013.
- J. Braun, M. Leonhardt, and J. M. Pawłowski (2018), arXiv: 1806.04432 [hep-ph].

Appendix

Transformed RG equation

- ▶ For $U^\dagger U = \mathbb{1}$ and $\partial_k U = 0$:

$$\begin{aligned}\frac{d\Gamma_k}{dk} &= \frac{1}{2} S\text{Tr} \left\{ \left[\Gamma_k^{(2)} + R_k \right]^{-1} \partial_k R_k \right\} \\ &= \frac{1}{2} S\text{Tr} \left\{ U U^\dagger \left[\Gamma_k^{(2)} + R_k \right]^{-1} U U^\dagger \partial_k R_k \right\} \\ &= \frac{1}{2} S\text{Tr} \left\{ \left[U^\dagger \Gamma_k^{(2)} U + U^\dagger R_k U \right]^{-1} \partial_k U^\dagger R_k U \right\} \\ &\equiv \frac{1}{2} S\text{Tr} \left\{ \left[\Gamma_{k;U}^{(2)} + R_{k;U} \right]^{-1} \partial_k R_{k;U} \right\}\end{aligned}$$

- ▶ With $\Gamma_{k;U}^{(2)} \equiv U^\dagger \Gamma_k^{(2)} U$ and $R_{k;U} \equiv U^\dagger R_k U$

- ▶ Three free model parameters: Yukawa coupling g and two meson potential UV initial conditions λ_Λ and v_Λ^2
 - ▶ To fix those we fit the quark mass M , the bare pion decay constant f_π and the sigma curvature mass m_σ

$$g = \frac{M}{f_\pi}$$

$$\lambda_\Lambda = \frac{m_\sigma^2}{2f_\pi^2} + 2I''_{0,\Lambda}(f_\pi^2)$$

$$v_\Lambda^2 = f_\pi^2 \frac{m_\sigma^2 - 4I'_{0,\Lambda}(f_\pi^2) + 4f_\pi^2 I''_{0,\Lambda}(f_\pi^2)}{m_\sigma^2 + 4f_\pi^2 I''_{0,\Lambda}(f_\pi^2)}$$

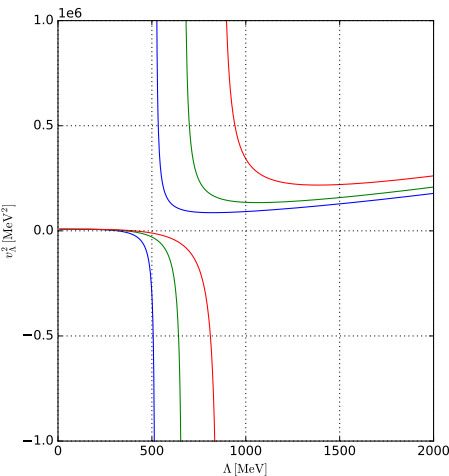
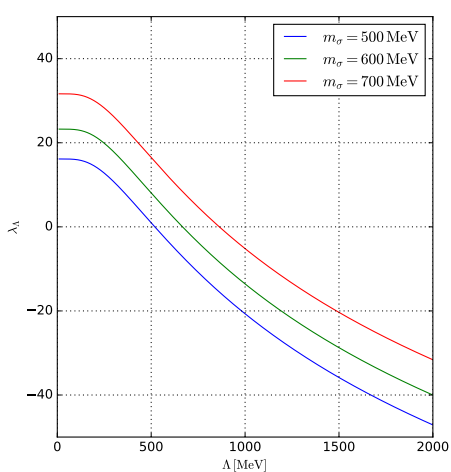
in vacuum with

$$l_{0,\Lambda}(\rho) \equiv \frac{1}{V_4} \int_{\Lambda}^0 dk \left(\text{Diagram} \right) \Big|_{\mu=T=q=0}$$

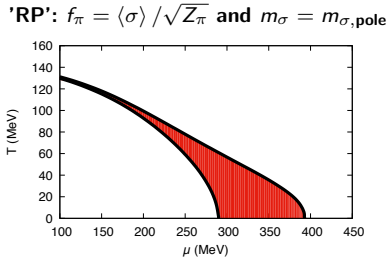
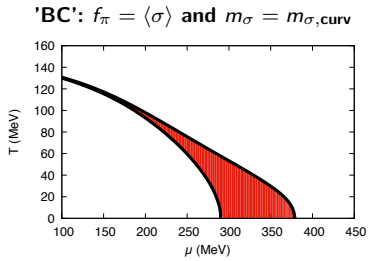
$$= \frac{2N_c}{\pi^2} \int_0^\infty p^2 dp \left(\sqrt{g^2\rho + p^2\lambda_0(p)^2} - \sqrt{g^2\rho + p^2\lambda_\Lambda(p)^2} \right)$$

Naïve parameter fixation

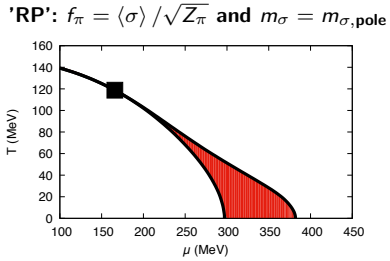
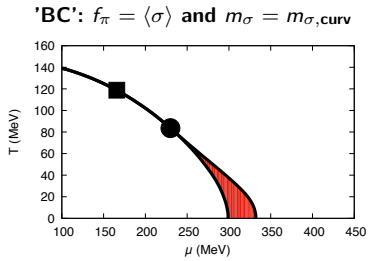
- ▶ $f_\pi = 88 \text{ MeV}$, $M = 300 \text{ MeV} \Rightarrow g(\Lambda) \cong 3.409 = \text{const.}$
- ▶ $\lambda_k^{\exp}(p)^2 = 1 + 1/(\exp(p^2/k^2) - 1)$



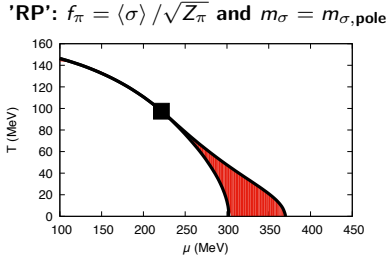
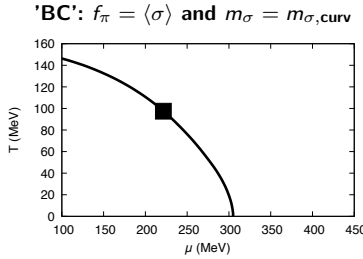
- MFA with *Pauli-Villars* (PV) regularization of the vacuum term with $\Lambda_{\text{PV}} = 0.2 \text{ GeV}$ ($f_\pi = 88 \text{ MeV}$, $M = 300 \text{ MeV}$, $m_\sigma = 2M$)



- MFA with *Pauli-Villars* (PV) regularization of the vacuum term with $\Lambda_{\text{PV}} = 0.3 \text{ GeV}$ ($f_\pi = 88 \text{ MeV}$, $M = 300 \text{ MeV}$, $m_\sigma = 2M$)



- MFA with *Pauli-Villars* (PV) regularization of the vacuum term with $\Lambda_{\text{PV}} = 0.4 \text{ GeV}$ ($f_\pi = 88 \text{ MeV}$, $M = 300 \text{ MeV}$, $m_\sigma = 2M$)

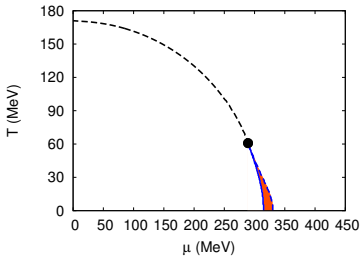


- MFA with RG regularization and MFA with PV-'BC' predict a **vanishing inhomogeneous window**

- MFA with *Pauli-Villars* (PV) regularization of the vacuum term with $\Lambda_{\text{PV}} = 5.0 \text{ GeV}$ ($f_\pi = 88 \text{ MeV}$, $M = 300 \text{ MeV}$, $m_\sigma = 2M$)

'BC': $f_\pi = \langle \sigma \rangle$ and $m_\sigma = m_{\sigma, \text{curv}}$

'RP': $f_\pi = \langle \sigma \rangle / \sqrt{Z_\pi}$ and $m_\sigma = m_{\sigma, \text{pole}}$



- MFA with RG regularization and MFA with PV-'BC' predict a **vanishing inhomogeneous window**
- MFA with PV-'RP' predict a **non-vanishing inhomogeneous window**

- ▶ C package for adaptive multidimensional integration (cubature) of vector-valued integrands over hypercubes

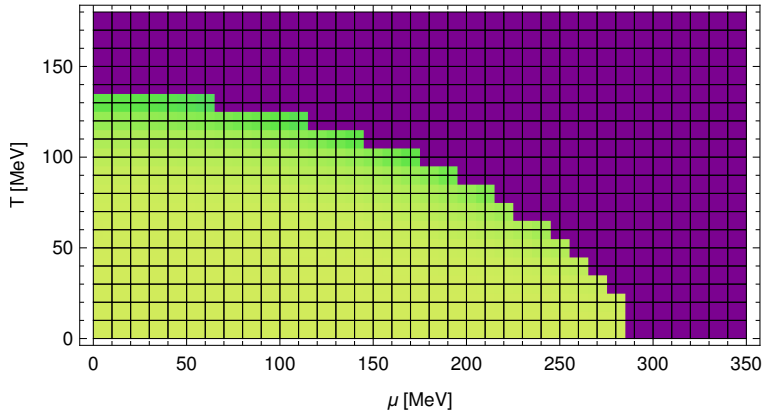
$$\int_{a_1}^{b_1} \int_{a_2}^{b_2} \cdots \int_{a_n}^{b_n} \vec{f}(\vec{x}) d^n x$$

- ▶ Free software under the terms of the GNU General Public License (v2 or later)
- ▶ **h-adaptive integration:** recursive partitioning the integration domain into smaller subdomains, applying the same integration rule to each, until convergence is achieved

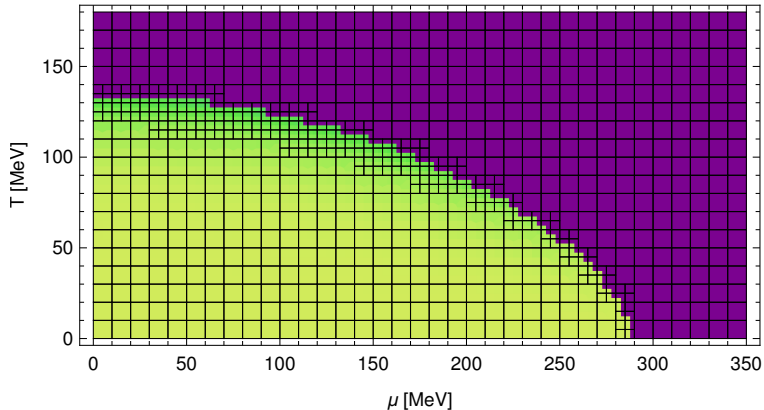
A. C. Genz and A. A. Malik, J. Comput. Appl. Math. (1980)

J. Berntsen, T. O. Espelid and A. Genz, ACM Trans. Math. Soft (1991)

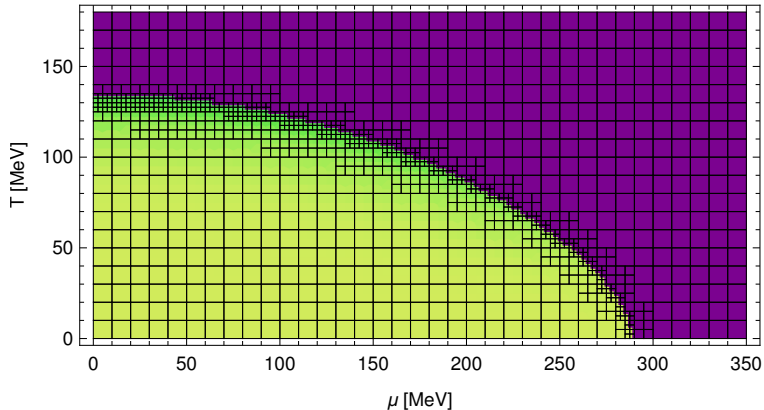
- ▶ Homogeneous sMFA (no vacuum term, no regularization) phase diagram
 $f_\pi = 88 \text{ MeV}$, $M = 300 \text{ MeV}$ and $m_\sigma = 600 \text{ MeV}$
- ▶ Mesh refinement based on the standard deviation of the order parameter on each tile
- ▶ 684 points, max resolution $10 \times 10 \text{ MeV}^2$, initial mesh



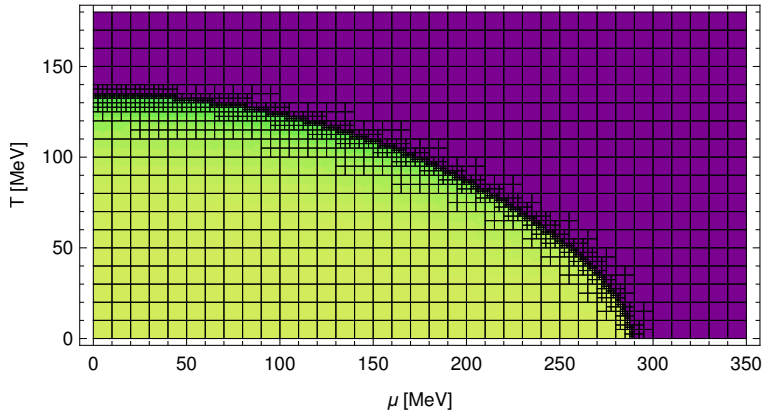
- ▶ Homogeneous sMFA (no vacuum term, no regularization) phase diagram
 $f_\pi = 88 \text{ MeV}$, $M = 300 \text{ MeV}$ and $m_\sigma = 600 \text{ MeV}$
- ▶ Mesh refinement based on the standard deviation of the order parameter on each tile
- ▶ 925 points, max resolution $5 \times 5 \text{ MeV}^2$, total saving factor 2.8



- ▶ Homogeneous sMFA (no vacuum term, no regularization) phase diagram $f_\pi = 88 \text{ MeV}$, $M = 300 \text{ MeV}$ and $m_\sigma = 600 \text{ MeV}$
- ▶ Mesh refinement based on the standard deviation of the order parameter on each tile
- ▶ 1419 points, max resolution $2.5 \times 2.5 \text{ MeV}^2$, total saving factor 7.6



- ▶ Homogeneous sMFA (no vacuum term, no regularization) phase diagram $f_\pi = 88 \text{ MeV}$, $M = 300 \text{ MeV}$ and $m_\sigma = 600 \text{ MeV}$
- ▶ Mesh refinement based on the standard deviation of the order parameter on each tile
- ▶ 2278 points, max resolution $1.25 \times 1.25 \text{ MeV}^2$, total saving factor 17.9



- ▶ Homogeneous sMFA (no vacuum term, no regularization) phase diagram
 $f_\pi = 88 \text{ MeV}$, $M = 300 \text{ MeV}$ and $m_\sigma = 600 \text{ MeV}$
- ▶ Mesh refinement based on the standard deviation of the order parameter on each tile
- ▶ 2278 points, max resolution $1.25 \times 1.25 \text{ MeV}^2$, total saving factor 17.9

